Eyelid Detection Method Based on a Fuzzy Multi-Objective Optimization

Yuniol Alvarez-Betancourt[1] and Miguel Garcia-Silvente[2]

[1] Department of Computer Sciences, University of Cienfuegos, Cuba

[2] Department of Computer Sciences and Artificial Intelligence, University of Granada, Spain

yalvarezb@ucf.edu.cu, m.garcia-silvente@decsai.ugr.es

Abstract. Iris recognition is one of the most robust human identification methods. In order to carry out accurate iris recognition, many factors of image quality should be born in mind. The eyelid occlusion is a quality factor that may significantly affect the accuracy. In this paper we introduce a new fuzzy multi-objective optimization approach based on the eyelid detection method. This method obtains the eyelid contour which represents the best solution of Pareto-optimal set taking into account five optimized objectives. This proposal is composed of three main stages, namely, gathering eyelid contour information, filtering eyelid contour and tracing eyelid contour. The results of the proposal are evaluated in a verification mode and thus a few performance measures are generated in order to compare them with other works of the state of the art. Thereby, the proposed method outperforms other approaches and it is very useful for implementing real applications as well.

Keywords. Eyelid detection, eyelid location, iris recognition, fuzzy systems, multi-objective optimization, combinatorial optimization.

Método de detección de parpados basado en un enfoque difuso de optimización multiobjetivo

Resumen. El reconocimiento del iris es considerado como uno de los métodos más robustos de identificación de humanos. Para realizar el reconocimiento con precisión se deben tener en cuenta varios factores de calidad de la imagen. La oclusión del párpado es un factor de calidad que afecta significativamente la precisión. En este artículo se presenta un nuevo método para detectar las oclusiones del párpado basado en un enfoque difuso de optimización con múltiples objetivos. Este método está compuesto por tres etapas principales: recopilación de información, filtrado y trazado del contorno del párpado. Los resultados del método propuesto son evaluados en un esquema de verificación y de esta forma se estiman algunas medidas de desempeño que son comparadas con otros trabajos del estado del arte. El método propuesto supera otros enfoques propuestos y resulta muy útil en la implementación de aplicaciones reales.

Palabras clave. Detección de párpados, localización de párpados, reconocimiento del iris, sistemas difusos, optimización multiobjetivo, optimización combinatorial.

1 Introduction

Iris recognition has gained more popularity in the last decade due to its interesting characteristics. This internal organ of the eye remains unalterable during our whole life and it is different and unique for each person (it even allows to distinguish twins). This biometric technology is also catalogued as one of the most robust human identification methods. Hence, many security sector companies have dedicated many efforts to introduce this technology in the market considering several areas. At the same time, numerous researchers are yet working hard to

overcome several open problems in this interesting research field [1-9].

A traditional iris biometric system is composed of 4 principal stages such as: image acquisition, preprocessing, feature extraction, and pattern matching [10]. The image acquisition stage begins by capturing a sequence of iris images from an individual using a special device (e.g., cameras, sensors) that operates in the visible spectrum or near infrared spectrum. A list of public image databases for research can be reviewed in the works [10, 11]. The preprocessing stage involves several steps: spoofing detection, iris location, image quality assessment, and normalization. In the feature extraction stage, most discriminant features are obtained from the textural content of the iris. This is based on encoding algorithms which have been developed using various approaches: discrete cosine transforms, ordinal features, scale-invariant feature transforms and multi-resolution analysis, among others. In order to complete pattern matching, several metrics are developed to measure the difference between two iris codes. The general aim of these stages relies upon digital image processing techniques, statistical techniques and artificial intelligence.

At present, the iris recognition tendency is expanding to other application areas in order to offer more flexibility. Therefore, biometric systems for environments with less constrains are required [1, 12, 13]. These environments add new drawbacks apart from the complexity already added in each mentioned stage. Likewise, major attention is demanded by the image preprocessing stage. This stage includes various steps: iris location, quality factors correction and normalization. The quality factors correction is a crucial step to improve the iris recognition accuracy. Thereby, images can be affected by different quality factors: defocus blur, motion blur, pupil dilation, pixel-counts, specular reflection, lighting, off-angle and occlusion [14]. In the case of image occlusions, they can be due to both the eyelashes and eyelids. This quality factor is very important because the extracted characteristics may not be enough in the subject identification stage. Also, occlusions may be partial or total. Generally, partial occlusions are fundamentally produced by the upper eyelid due to the people's natural aging process. The total occlusion is due to illness, lighting change or environmental change which causes people to close their eyes.

The eyelid occlusion is a quality factor widely studied but it still demands more attention in order to improve the performance of the iris recognition systems. Many of the eyelid detection methods proposed have used line fitting, parabolic curve fitting, searching using line Hough transform or parabolic Hough transform and combinations of them. Likewise, a so-called integro-differential operator was defined by Daugman [8] to locate the iris and to exclude the eyelids modeled as fitted circular contours. Besides, Li proposed a method which combines a parabolic integro-differential operator and a RANSAC (RANdom SAmple Consensus) technique [15]. To this end, Cui [9] proposed an eyelid detection approach using parabolic curve fitting based on gray value segmentation. In this sense, Rossant developed a more robust method to detect eyelids which applies a few preprocessing steps and later uses gradient maximization to model eyelids with curve fitting in regions of interest [3]. Roy [1] used parabolic curve fitting to detect eyelids as well. Tae [5] presented an automatic eyelid and eyelash detection method based on the parabolic Hough model and Otsu thresholding method. Libor Masek [16] delimited the iris regions and eyelids by horizontal lines which were approximated to upper and lower eyelid boundaries using a lineal Hough transform. A novel coarse-line to fine-parabola eyelid fitting scheme was proposed by He to detect eyelids localization [6]. Moreover, a method to detect eyelid based on fitting straight lines using data of linear Hough transform was proposed by Liu [17].

The line Hough transform has less parameters than the parabolic one and hence is very useful when a system requires low computation time. However, the parabolic Hough transform is more effective than the lineal transform to model the eyelid shape due to the parabolic shape of the eyelids. Other important element to consider is the way those parameters or data for modeling the eyelid are obtained. In most cases, the parameters are gathered with low preprocessing which produces the detection of unsuited eyelid contours. Generally, the area of eyelid is affected by defocus, eyelashes and other occlusions like

the use of glasses. Therefore, the recovering of data to model the eyelid shape requires a special processing.

In this paper, we propose a novel and accurate method to detect the eyelid occlusions. It is based on a fuzzy multi-objective optimization approach. That approach is composed by three principal stages: gathering eyelid contour information, filtering eyelid contour and tracing eyelid contour. The two first stages apply spatial transformations and the proposed horizontality principle to obtain a set of candidate pieces for eyelid contour. The last stage deals with a fuzzy multi-objective optimization framework to obtain the Pareto-optimal set of eyelid contour pieces combinations taking into account five well defined objectives. Finally, three of these objectives are subject to constrains. This framework is based on an arbitrary combinatorial optimization process. Besides, a Mamdani's fuzzy inference system is used to select the best solution of the Pareto-optimal set as the best combination of contour pieces that represent the eyelid contour. The results of the proposal are reliable and very competitive with respect to the state of the art in terms of accuracy.

The remainder of this paper is structured as follows. Section 2 presents the used method to locate the iris. Section 3 introduces the proposed eyelid detection method. The experiments and the results of applying the proposal are exposed in Section 4.

2 Iris Location

The iris is an internal organ of the eye located behind the cornea and the aqueous humor. It consists of a weave of connective tissues, fibers, rings and colors. These constitute a distinctive and unique mark of people when iris is observed from a short distance [10]. Besides, as a visible feature we can see a sinuous structure, so-called collarette, surrounding the pupil region. Also, a cumulus of structural features is visible in the iris which can be classified in two categories [10]:

- Features that relate to the pigmentation of the iris (e.g., pigment spots, pigment frill).
- The movement-related features, in other words, features of the iris relating to its function as pupil size control (e.g., iris sphincter, contraction furrows, radial furrows).

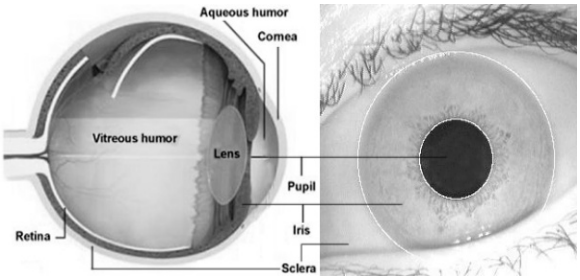

Fig. 1. Structure of human eye

Furthermore, if the iris is observed from the center of the circle which models the inner boundary up to its outer boundary, two delimiting borders can be identified (see Fig. 1). The first one, pupil-iris, is defined by the shift of the intensity lower values (pupil area) of the image to middle intensities which characterize the iris region. The second border, iris-sclera is characterized by the shift of middle values of intensity to the highest values (sclera area) of the image. Besides, its geometric character (circular or elliptical shape depending on the point of view) constitutes another characteristic of great importance for automatic detection.

Most of the approaches for iris location exposed in the specialized bibliography have as their main objective the search of circular objects inside images.

Considering previous assumptions, in this work we use the iris location method which has been proposed by the authors in an earlier work [4]. That method is composed of two principal stages. The first one intends to obtain an initial approximation of the center $P(X_0, Y_0)$ of the circle which models the pupil boundary by the use of a sequence of basic image processing techniques. The second stage tries to find the circular boundary which represents the best inner or outer boundary of the iris from the obtained initial approximation of the center. In this way, that search problem is formulated to determine the radius $r_s^* \in R$, $R = \{r_{\min}, r_{\min}+1, ..., r_{\max}-1, r_{\max}\}$ of the circle with center $P(X_0, Y_0)$ such as

$$r_s^* = \arg\max_{r \in R} D_s(r)$$

$$D_s(r) = F_{\substack{QMA \\ (x_i,y_i)\in C_s(r,X_0,Y_0)}}\left(\frac{\partial f(x_i,y_i)}{\partial s}\right) = \quad (1)$$

$$F_{\substack{QMA \\ (x_i,y_i)\in C_s(r,X_0,Y_0)}}\left(f\left(x_i+\Delta_{sx_i},y_i+\Delta_{sy_i}\right)-f(x_i,y_i)\right). \quad (2)$$

It is worth to mention that F_{QMA} refers to the quantified majority operator QMA-OWA which is explained in more detail in our earlier work [4]. Also, $f(x_i,y_i)$ represents the intensity of a pixel of the image F in coordinates (x,y). Besides, $C_s(r,X_0,Y_0)$ stands for the set of points of interest belonging to the semi-circumference in the sense $s \in S$, $S=\{left,right,top,bottom\}$. See [4] for further details of this iris location approach.

3 Eyelid Detection

The proposed eyelid detection method is based on a fuzzy multi-objective optimization approach with constrains. An initial part of that method is related with the gathering of eyelid contour information. In this stage some spatial operations over the raw image are executed. Afterwards, a horizontal principle is applied to achieve the most relevant eyelid contour information. Hence, the obtained contour information is formed by pixels which are the closest or coming from the original eyelid contour. In this way, each pixel is labeled using a search procedure of eight connected components. The labeled pixels are candidate members for eyelid contour pieces. The last part of the method is tracing eyelid contour. This is based on the selection of the best combination of eyelid contour pieces by the use of a fuzzy multi-objective optimization approach.

3.1 Gathering Eyelid Contour Information

The recovering of eyelid contour information is a very important step to make a good eyelid contour

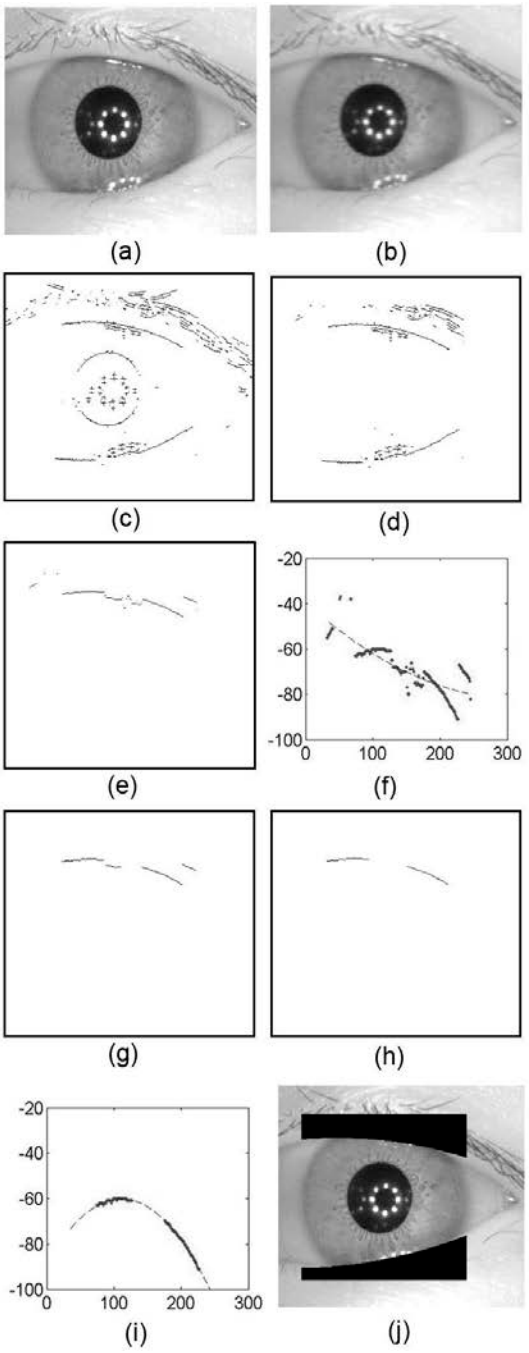

Fig. 2. (a) Raw image. (b) Smoothed image. (c) Detected contours. (d) Eyelid parts. (e) Top eyelid contour obtained with the profile operation. (f) Graph with the obtained candidate points. (g) Filtered image. (h) Eyelid contours pieces. (i) Graph with eyelid points. (j) Resultant eyelids detection

detection. In a first moment two spatial operations are applied to highlight the eyelid contour. The first one is a Gaussian lowpass filter which is applied to mitigate the adverse effects of noise (see Fig. 2(b)). After certain amount of trial and error, we determined that lowpass filter is well suited with a convolution mask 3 X 3 and standard deviation $\sigma = 1$. The second one is a horizontal Sobel filter. This Sobel filter returns a binary image with the horizontal contours highlighted as shown in Fig. 2(c).

Later, we extract the top and bottom iris parts to detect the eyelid occlusion. The delimitation of these two regions in order to detect the top and the bottom eyelids is a main issue to considerably reduce the computational time.

The result of applying both procedures is shown in Fig. 2(d). The proposed eyelid detection method is applied on each part of the iris. Thereby, we start the recovering of eyelids pieces with a profile operation in the top and bottom parts. For example, for the top eyelid part a profile operation is executed from the inner iris boundary to the top outer iris boundary. In this way, that procedure is applied to each consecutive pixel in the direction left to right obtaining the first pixel distinct of zero in each profile. Likewise, a profile operation from the inner iris boundary to the bottom outer iris boundary in the direction left to right is performed for the bottom eyelid detection. In a more explicit way, the reader can see in Fig. 2(e) an example of the gathering eyelid contour information in the top eyelid region. Also, Fig. 2(f) shows a graph with the obtained candidate points and the fit of those points with a second-order parabolic curve.

3.2 Filtering Eyelid Contour

After the profile operation, a contour filter is applied in both delimited regions. This filter sets up a horizontality principle which must be reached by each candidate piece for the eyelid contour. It is important to point out that the formal definition of this horizontality principle is motivated by the success of similar techniques proposed earlier [3]. Thereby, every contour is labeled and thus is grouped in the set $H = \{h_1, h_2, ..., h_n\}$. Later, we can execute the horizontality principle in the delimited regions. In essence, each h_i will belong to the final candidate pieces set $S = \{s_1, s_2, ..., s_m\}$ for the eyelid contour, only if the following conditions are satisfied:

- $Rd^i < \frac{Cd^i}{2}$,

- $Cd^i \geq M_{cd}, M_{cd} = \frac{1}{n}\sum_{i=1}^{n} Cd_i$,

where Rd^i is the difference between max and min rows of the contour labeled as h_i. Likewise, Cd^i is the difference between max and min columns of the contours labeled as h_i.

Accordingly, Fig. 3 shows a graphical representation of that horizontality concept. This figure depicts 3 cases of the proportions which are required to apply the previous conditions. These cases vary in respect to the extension of the contours considering the rows. Besides, this graph intends to explain in a more graphical way, the condition of the proportion between columns and rows extension of each horizontal contours.

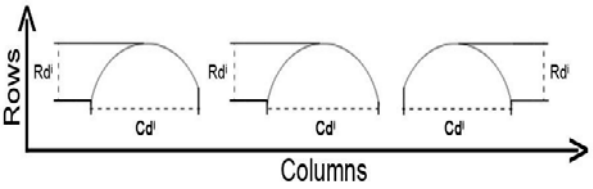

Fig. 3. Graphical representation of the horizontality principle

3.3 Tracing Eyelid Contour

Consequently, the regions of interest of the image are ready to accomplish the tracing eyelid contour based on the fuzzy multi-objective optimization approach. The tracing eyelid contour stage is conceived in an arbitrary optimization context with five objectives which are maximized or minimized depending on the specific objectives and all are equally important. Besides, three of these objectives are subject to constrain.

To this end, the process starts with the outline of the search space which consists in obtaining all possible combinations of candidate pieces s_i for

eyelid contour. In this sense, each s_i obtained earlier is labeled with numbers between 1 and the size of the set S. Afterwards, all possible combinations of labeled elements s_i are obtained and defined as the set $C = \{c_1, c_2, ..., c_w\}$. Notice that in the combinatorial process, each combination created by $k\ (2 \le k \le n)$ different elements of a set of n elements may be called a combination of n elements. A combination is considered only if it is composed of at least one different element with respect to all other combinations.

Considering all these annotations, the multi-objective problem can be formulated. We present the details of the problem formulation to detect the combination c_i of candidate pieces for contour which best models the eyelid contour. Thereby, the objective functions to be reached are:

- $f_1(c_i) = \arg\max Size(c_i)$, *where* $Size(c_i)$ *is the* amount of pixels which compose c_i;

- $f_2(c_i) = \begin{cases} \arg\max A & ; \ c_i \in Top\ eyelid \\ \arg\max -A & ; \ c_i \in Bot\ eyelid \end{cases}$, where A is a coefficient of the equation $A\left(col_j^i\right)^2 + Bcol_j^i + |C| = row_j^i$ which fits the positions of the pixels of c_i with the least squares method;

- $f_3(c_i) = \arg\min MSE(c_i)$, where $MSE(c_i)$ represents the mean square error of the fitting (using the least squares method) of the positions of the pixels of c_i;

- $f_4(c_i) = \underset{row_j^i \in c_i}{\arg\min}\, Mean\left(\frac{\partial c_i}{\partial row_j^i}\right)$, where row_j^i are the row positions of the pixels of c_i and $Mean\left(\frac{\partial c_i}{\partial row_j^i}\right) = \frac{1}{m}\sum_{j=1}^{m-1}\left|row_j^i - row_{j+1}^i\right|$;

- $f_5(c_i) = \underset{col_j^i \in c_i}{\arg\min}\, Mean\left(\frac{\partial c_i}{\partial col_j^i}\right)$, where col_j^i are the column positions of the pixels of c_i and $Mean\left(\frac{\partial c_i}{\partial col_j^i}\right) = \frac{1}{m}\sum_{j=1}^{m-1}\left|col_j^i - col_{j+1}^i\right|$.

The objective functions f_1, f_2 and f_3 are subject to constrains to delimit the feasible search space and hence to reduce the computational cost looking for the optimal solution set. Now, the success of finding the optimal search space depends significantly on the selection of the adequate constrain parameters.

Consequently, the set of constrains established are the following:

- $f_1 : Size(c_i) > L$, where L was selected experimentally as a third part of a delimited region length;

- $f_2 : A(c_i) = \begin{cases} A > 0; & h_i \in Top\ eyelid \\ A < 0; & h_i \in Bot\ eyelid \end{cases}$;

- $f_3 : MSE(c_i) < T$, where $T = 20$ was selected empirically by observing the behavior of all fitted curves.

With the objective functions and their respective defined constrains, we can accomplish the search of the optimal solutions in the set C. That search is executed taking into account the concept of dominance (as the most multi-objective optimization algorithms). The dominance concept summarizes the conditions to decide if a solution is better eligible than the other one. Likewise, the concept of dominance is herewith defined.

Definition: A solution $x^{(1)}$ is said to dominate the other solution $x^{(2)}$, if both conditions 1 and 2 which follows are true.

1. The solution $x^{(1)}$ is not worse than $x^{(2)}$ in all objectives: $f_j(x^{(1)}) \not\succ f_j(x^{(2)})$, for all $j = 1, 2, ..., M$;

2. The solution $x^{(1)}$ is strictly better than $x^{(2)}$ in at least one objective: $f_{\bar{j}}(x^{(1)}) \lhd f_{\bar{j}}(x^{(2)})$ for at least one $\bar{j} \in \{1, 2, ..., M\}$ where $M = 5$ is the amount of objective functions discussed above.

Henceforth, we explain how to look for the best solutions according to the objectives and constrains presented earlier. For a given finite set of solutions $C = \{c_1, c_2, ..., c_w\}$ previously delimited with the defined constrains, we can perform all possible pairwise comparisons and find which solutions are non-dominated with respect to each other. This algorithm, which looks for all non-dominated solutions, is proposed in [18]. In more detail, to find the best non-dominated front, the domination concept is checked in every solution from the population (the set of solutions C) with a partially filled population. Let us denote C as the population and P as the partially filled population. When all solutions of the population are checked, the remaining members of P constitute the non-dominated front (the Pareto-optimal set). This requires a maximum of $N(N-1)/2$ domination checks, where N is the size of the set C. For further details of the described method, you can see the pseudocode which follows.

As it was mentioned before, we expect to have a non-dominated front of solutions P according to the formalized problem. For any solution outside of this set, we can always find a solution in this set which will dominate the first one. Thus, this particular set has a property of dominating all other solutions which do not belong to this set. In simple terms, this means that the solutions of this set are better compared to the rest of solutions. Now the question is how to select the best solution in P. It requires an assessment with respect to one or various objectives which have more influence over the eyelid contour detection.

To this end, we propose to implement a decision maker based on a Mamdani's fuzzy inference system. Hence, we can detect automatically what p_i has the best membership to the fuzzy concept of eyelid contour. Fuzzy inference is the process of formulating a mapping from a given input to an output using fuzzy logic. The mapping then provides the basis for making decisions. The process of fuzzy inference involves several issues such as fuzzification of the input variables and design of if-then rules base. Those elements should be carefully formulated to obtain the feasible results as required.

Pseudocode 1: Eyelid detection method

```
1:  Obtain S set of eyelid contour pieces
2:  Obtain C set of all combination of s_i
3:  Apply constrains to C set
4:  Initialize P_1 = C_1
5:  Initialize flag = false
6:  for h = 2 to size of C do
7:     for k = 1 to size of P do
8:        if C_h dominates P_k then
9:           Delete P_k from P
10:       else if P_k dominates C_h then
11:          flag = true
12:          Break for
13:       end if
14:    end for
15:    if flag == false then
16:       Insert C_h in P
17:    else
18:       flag = false
19:    end if
20: end for
21: Apply decision maker to P
```

In the proposed decision maker, input variables correspond to the 5 features measured to maximize or minimize objective functions. Thus, let us denote every variable: length $Length(p_i)$, curvature coefficient $Curvature(p_i)$, mean square error $MSE(p_i)$, mean of row differences $MRD(p_i)$ and mean of column differences $MCD(p_i)$.

For each variable of p_i, a normalization procedure was executed to map the crisp values to fuzzy values through the respective membership functions. The normalization process consists of scaling all variables to the range $[0,1]$. These normalized values are calculated dividing the *j*-th variable of *i*-th non-dominated solution by the maximum value of that *j*-th variable obtained in the set C. This normalization can be formulated as follows:

$$VariableN^j(p_i) = \frac{Variable^j(p_i)}{\max(Variable^j(C))} \ .$$

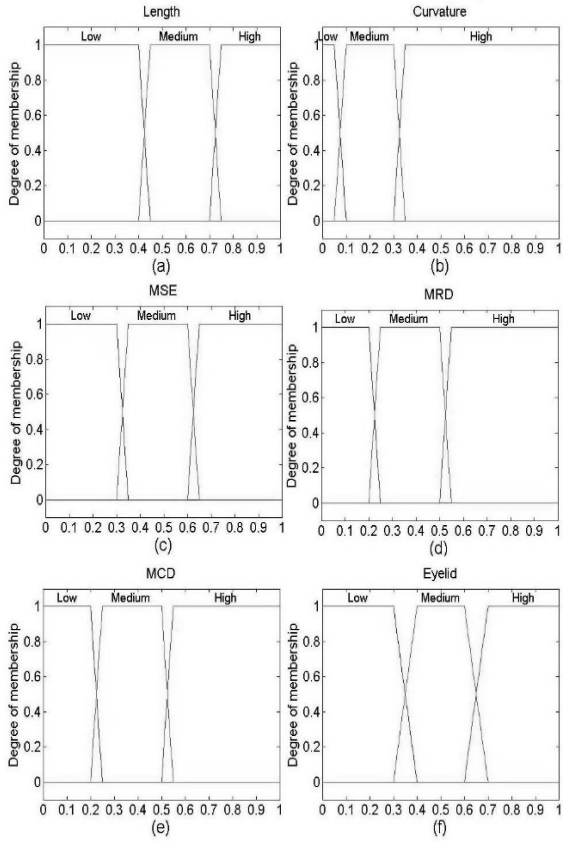

Fig. 4. Membership functions

The design of membership functions is another important element in the fuzzification of input variables. Thus, all the membership functions were modeled as trapezoidal (see Fig. 4). This type is one of the simplest membership functions and hence its computational complexity is low. A full revision of the behavior of all variables measured in C was accomplished to estimate the parameters of each trapezoidal membership function. That revision enables us to carry out an adequate parameterization based on subjective classification of percentages.

Furthermore, a wide base of if-then rules was developed. This base of rules was conceived to deal with a great number of occurrences. The base of rules is exposed in Table 1. All rules are evaluated in parallel using fuzzy inference and the results are combined and defuzzified. Likewise, the membership degree of each p_i to the fuzzy concept is obtained and is denoted as $EC(p_i)$. The membership function designed for the fuzzy concept is shown in Fig. 4(f).

Table 1. Base of if-then rules to describe the fuzzy concept of eyelid contour

INPUT VARIABLES									OUTPUT
LENGTH		CURVATURE		MSE		MRD		MCD	EYELID
H	&	H	&	L	&	L	&	L	H
H	&	M	&	L	&	L	&	L	H
H	&	M	&	M	&	L	&	L	H
H	&	M	&	M	&	M	&	L	M
H	&	M	&	M	&	M	&	M	L
H	&	H	&	M	&	L	&	L	H
H	&	H	&	M	&	M	&	L	H
H	&	H	&	M	&	M	&	M	M
H	&	H	&	L	&	M	&	L	H
H	&	H	&	L	&	M	&	M	H
H	&	H	&	L	&	L	&	M	H
M	&	H	&	L	&	L	&	L	H
M	&	M	&	L	&	L	&	L	H
M	&	M	&	M	&	L	&	L	M
M	&	M	&	M	&	M	&	L	L
M	&	M	&	M	&	M	&	M	L
M	&	H	&	M	&	L	&	L	H
M	&	H	&	M	&	M	&	L	M
M	&	H	&	M	&	M	&	M	L
M	&	H	&	L	&	M	&	L	H
M	&	H	&	L	&	M	&	M	M
M	&	H	&	L	&	L	&	M	H
L	or	L	or	H	or	H	or	H	L

Finally, the selection of the solution p_i which corresponds to the best eyelid contour approximation is summarized to detect the maximum value of the membership to fuzzy concept $EC(p_i)$. Fig. 2(h) presents the non-dominated solution corresponding to the best eyelid contour. Likewise, Fig. 2(i) shows a graph

with the obtained points of eyelid contour pieces and the curve fitted by those points of a second-order function (the curve). In addition to this, Fig. 2(j) presents an example of top and bottom eyelid detection which has highlighted the eyelids with a shaded black region.

4 Experiments and Results

With the aim to validate the performance of the proposed eyelid detection method, an experimentation phase was developed. The experiments were executed using a Core 2 Duo laptop computer at 2.2 GHz with 4GB of RAM memory. The image database CASIA-IrisV4-Interval was utilized as input data. This image database is considered a standard for iris research and was provided by The Chinese Academy of Sciences - Institute of Automation (CASIA) [19]. The images were captured for the iris recognition research using specialized digital optics developed by the National Laboratory of Pattern Recognition, China. Images from each class were taken from two sessions with one month interval between sessions. CASIA-IrisV4-Interval is a superset of CASIA V1.0 and contains 2639 gray scale eye images with 395 classes. In the acquisition stage by the NIR illumination scheme used, many specular reflections in the pupil of each image eye were generated (see Fig. 2(a)). Another interesting element to mention is the influence of eyelid occlusions. This quality factor affects the whole database in a large measure. The detection of this factor is very important to improve the iris recognition accuracy. Fig. 5 presents a few results of the proposed eyelid detection method.

Besides, it is important to point out that having as base the Daugman algorithm implemented in MatLab by Libor Masek [16] and modifying the segmentation module, the proposed algorithm is executed. Due to this reutilization of Libor source code for the iris normalization and feature extraction stages, the iris recognition accuracy can be estimated. This code accomplishes iris normalization through the Daugman's Rubber Sheet Model [8]. The feature extraction stage is executed by convolving the normalized iris pattern

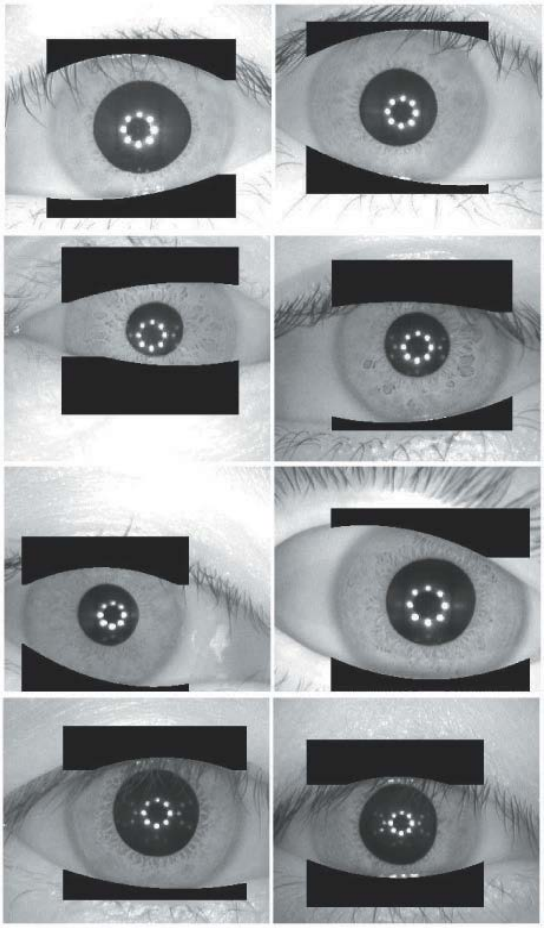

Fig. 5. Successful results of the proposed eyelids detection method

with 1D Log-Gabor wavelets and the pattern matching stage uses the Hamming distance.

Thus, the experimentations were conceived in a verification mode. In the verification mode the claim of the identity of a person presented to the system (the entry iris feature vector of the person) is matched with the claimed person prototype model (in our case, the mean feature vector of the iris feature vectors acquired during enrolment) just as it was proposed by Vitomir and Nikola [20]. Hence, if the entry iris feature vector and the mean feature vector of the claimed identity have a degree of similarity (measured with Hamming distance) that is lower than the system threshold L_0, then the claim is accepted, otherwise, the claim is rejected (or vice versa if a dissimilarity

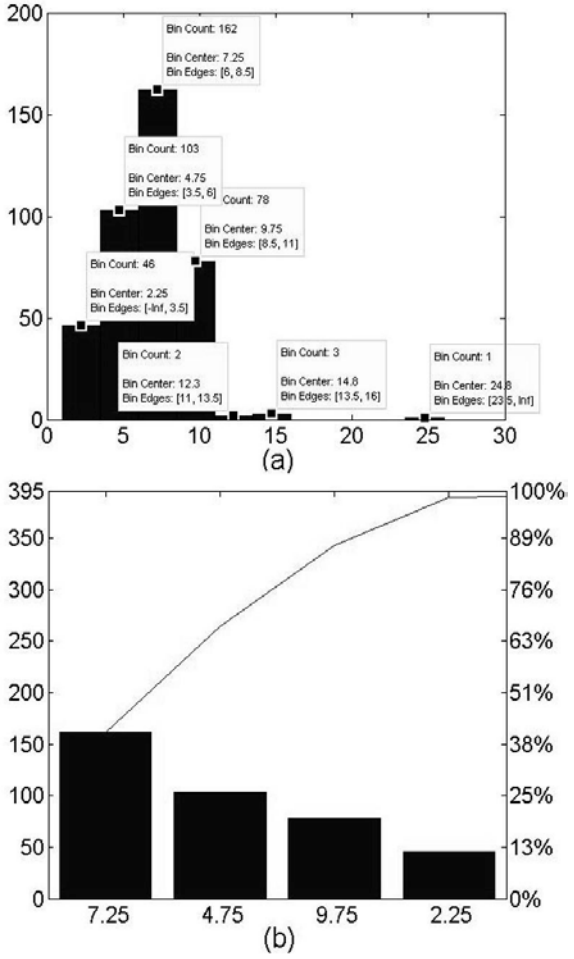

Fig. 6. Distribution of instances per class in CASIA-IrisV4-Interval dataset

measure is used). In this way, we use the performance measures in terms of the Genuine Accept Rate $GAR = 100 - FRR$, False Reject Rate $FRR = 100 * (n_{rc} / n_c)$, False Accept Rate $FAR = 100 * (n_{ai} / n_i)$ and Equal Error Rate (value obtained when FRR and FAR are equal). Let us denote n_{rc} as the number of rejected genuine identity claims, n_c as the number of all genuine identity claims made, n_{ai} as the number of accepted non-genuine identity claims and n_i as the number of all non-genuine identity claims made. The FAR and FRR are measures which are directly correlated to the threshold L_0; if it is increased to make the system more tolerant to input variations, then FAR increases. Otherwise, if L_0 is decreased to make the system more reliable, then FRR increases.

First of all, an image selection process is required to execute the experimentations because the CASIA dataset is composed of imbalanced classes. Hence, a histogram operation is accomplished to show the distribution of the instances per class. As the data input, we gather the count of instance per class in a vector and this vector is partitioned into 10 equally spaced containers to obtain the histogram. Fig. 6(a) presents the histogram with details of the seven best containers. The other instances-distribution measure is shown in Fig. 6(b). This chart displays the first 95% of the cumulative distribution of bin count as bars drawn in descending order.

Having performed these two types of instances-distribution analyses we arrive to the following conclusion. To execute the experimentations of this work it is recommended to select those classes which contain 5 or more instances per class. There exist 338 classes which satisfy this condition. Such classes represent an 85.57% of the 395 classes. Also, these classes sum a total of 2512 images which represent a 95.19% of the 2639 images of the CASIA dataset.

In order to show the good performance of the proposed eyelid detection method, each class is partitioned in two sets, train and test instances. Therefore, the first 4 instances per class are selected to train the model of classification and the other instances of each class are used as test instances. With these assumptions, firstly we explore two variants of the proposed method with the aim to obtain a well suited trade-off between the computational cost and accuracy. The first one is denoted as Method 1 which consists of applying the fuzzy concept to each element of the $C = \{c_1, c_2, ..., c_w\}$ set and thus to obtain a decision on each tested image regarding the combinations which model the top and bottom eyelid. The second variant stands for Method 2 which represents the complete process we propose (the search for the Pareto-optimal set of combination

Table 2. Comparison of computational time and accuracy for the two analyzed variants

Methods	Time in seconds			Accuracy at EER
	Min	Max	Mean	
Method1	0.22	1.82	0.37	97.44%
Method2	0.23	1.92	0.38	97.93%

followed by the decision making process using the fuzzy concept).

To this end, we obtain two vectors which represent the results of applying the variants on the entire image database. Besides, in order to prove the differences between the two methods a Kolmogorov-Smirnov test is accomplished. This hypothesis test tries to demonstrate if two samples come from the same continuous distribution (null hypothesis H_0), against the alternative that they do not come from the same distribution (alternative hypothesis H_1). The result rejects the null hypothesis at the 5% significance level. Hence, it is interesting to execute another test to decide which one of the two analyzed methods is most reliable. To this goal, the computational cost in terms of consuming time of each method is analyzed and shown in Table 2. Also, the accuracy at EER is shown in that table.

As we can see in the previous table, Method 1 has the lowest time; however, it does not reach the best accuracy. Method 2 acquires more accuracy at EER than the accuracy of Method 1, but it is not significant. Hence, a more complete analysis is carried out as it is shown in Fig. 7(a). This figure depicts the performance curves of Detection Error Trade-off (DET) type in which the best curve has the least area under the curve. This graph plots the False Accept Rate versus False Reject Rate. Also, the points of EER in the two curves are linked with a diagonal black line as it is shown in the graph. In this way, we can observe that Method 2 experiments more global robustness. Therefore, we select Method 2 to develop the experimentation on the influence of the correct eyelid detection to improve the iris recognition accuracy.

With these assumptions, we discard the images affected with an occlusion percentage

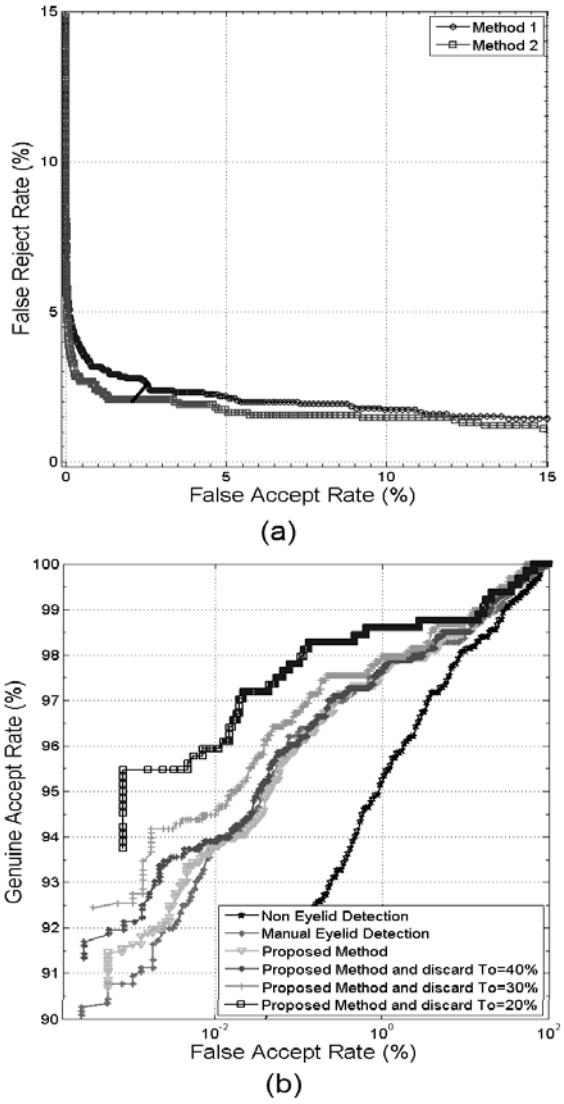

Fig. 7. (a) DET performance curves. (b) ROC performance curves

over a threshold T_o and different performance measures can be obtained. Also, these results are compared with the results of non-eyelid detection and manual eyelid detection by using performance curves. Fig. 7(b) shows other performance curve of Receiver Operator Characteristic (ROC) type which exposes the successful results of the proposal respect to other experimentation variants. These types of curve plot the False Accept Rate against Genuine

Table 3. Comparison with the state of the art

Methods	Accuracy at EER	Accuracy at FAR=0.00%
Daugman [8]	99.33%	96.59%
Proposed method	**98.59%**	**95.94%**
Manual Eyelid Detection	97.93%	93.79%
Sun [21]	97.87%	94.00%
Rahulkar [2]	97.81%	95.79%
Non-Eyelid Detection	96.74%	85.68%
Monro [7]	95.73%	86.67%

Accept Rate and the best curve is the one which maximizes the area under the curve. In that graph, we can see how EER decreases from 3.26% (non-eyelid detection) to 1.41% (proposed method and discard T_o=20%). Thereby, significant improvements are obtained on the iris recognition performance when our proposal is applied and the images more affected by occlusions are discarded.

Furthermore, we compare the proposed method with other well-known works of the state of the art. Thus, the accuracy values of that works are taken from [2] whose results are high and may serve as ground truth. These results are obtained with experimentations with similar characteristics with respect to our proposal. They are also evaluated over CASIA dataset. Likewise, Table 3 shows the accuracy in terms of Equal Error Rate (EER) and $FAR = 0.00\%$. Besides, the results of non-eyelid detection and manual eyelid detection are compared with the proposal as well.

As it was shown in Table 3, our proposal of discarding the images with occlusions over 20% is very competitive with respect to the best performance obtained by Daugman [8]. Thus, the best performance for EER is 99.33% and our work reaches an accuracy of 98.59% which outperforms the rest of proposals. As future work, the performance could be improved by adding some approaches to detect other quality factors such as specular reflections, eyelashes occlusions and blurred images which affect in great measure the CASIA-IrisV4-Interval dataset.

5 Conclusions

In this paper, a new eyelid detection method based on a fuzzy multi-objective optimization approach is presented. To accomplish this approach three processing stages are conceived, namely, gathering eyelid contour information, filtering eyelid contour and tracing eyelid contour. We focused on the last one, so our proposal deals with a fuzzy multi-objective optimization framework to obtain the Pareto-optimal set of eyelid contour pieces combinations taking into account five well defined objectives. In that way, a Mamdani's fuzzy inference system is deployed to select the best solution of the Pareto-optimal set as the best combination of contour pieces that represent the eyelid contour in each eyelid region. This new proposal is efficient with respect to computational time. Besides, the performance reached is very competitive compared to the state of the art. Also, it is proven that when occluded images of CASIA-IrisV4-Interval dataset having an occlusion percent higher than 20% are discarded, the performance can be significantly improved. Our proposal obtains an accuracy of 98.59% which outperforms other works on iris recognition. Finally, we may conclude that our proposal is very useful for any iris recognition system and suitable to be implemented in real applications.

Acknowledgements

This work was supported by Andalusian Regional Government project P09-TIC-04813, the Spanish Government project TIN2012-38969 and by the AUIP. Besides, the authors would like to thank the Chinese Academy of Sciences, Institute of Automation (CASIA) from Beijing, China, for their gracefulness in allowing us to use the CASIA-IrisV4 Images Data Base in our experiments.

References

1. **Roy, K., Bhattacharya, P., & Suen, C.Y. (2011).** Towards nonideal iris recognition based on level set method, genetic algorithms and adaptive asymmetrical SVMs. *Engineering Applications of Artificial Intelligence*, 24(3), 458–475.

2. **Rahulkar, A.D., Jadhav, D.V., & Holambe, R.S. (2011).** Fast discrete curvelet transform based anisotropic iris coding and recognition using k-out-of-n: A fused post-classifier. *Machine Vision and Applications*, 23(6), 1115–1127.
3. **Rossant, F., Mikovicova, B., Adam, M., & Trocan, M. (2010).** A Robust Iris Identification System Based on Wavelet Packet Decomposition and Local Comparisons of the Extracted Signatures. *EURASIP Journal on Advances in Signal Processing*, 2010, article No. 12.
4. **Alvarez-Betancourt, Y. & Garcia-Silvente, M. (2010).** A fast Iris Location based on aggregating gradient approximation using QMA-OWA operator. *2010 IEEE International Conference on Fuzzy Systems*, Barcelona, Spain, 1–8.
5. **Tae-Hong, M. & Rae-Hong, P. (2009).** Eyelid and eyelash detection method in the normalized iris image using the parabolic Hough model and Otsu's thresholding method. *Pattern Recognition Letters*, 30(12), 1138–1143.
6. **He, Z., Tan, T., Sun, Z., & Qiu, X. (2008).** Robust Eyelid, Eyelash and Shadow Localization for Iris Recognition. *15th IEEE International Conference on Image Processing (ICIP 2008),* San Diego, CA, 265–268.
7. **Monro, D.M., Rakshit, S., & Zhang, D. (2007).** DCT-based iris recognition. *IEEE Transactions Pattern Analysis and Machine Intelligence*, 29(4), 586–595.
8. **Daugman, J. (2004).** How iris recognition works. *IEEE Transactions on Circuits and Systems for Video Technology*, 14(1), 21–30.
9. **Cui, J., Wang, Y., Tan, T., Ma, L., & Sun, Z. (2004).** A fast and robust iris localization method based on texture segmentation. *SPIE 5404*, *Biometric Technology for Human Identification*, Orlando, FL, 401–408.
10. **Li, S.Z. & Jain, A.K. (2009).** Encyclopedia of Biometrics, New York: Springer.
11. **Bowyer, K.W., Hollingsworth, K., & Flynn, P.J. (2008).** Image understanding for iris biometrics: A survey. *Computer Vision and Image Understanding*, 110(2), 281–307.
12. **Li, P., & Ma, H. (2012).** Iris recognition in non-ideal imaging conditions. *Pattern Recognition Letters*, 33(8), 1012–1018.
13. **Zuo, J. & Schmid, N.A. (2010).** On a methodology for robust segmentation of nonideal iris images. *IEEE Transactions on Systems, Man, and Cybernetics, Part B: Cybernetics*, 40(3), 703–718.
14. **Kalka, N.D., Zuo, J., Schmid, N.A., & Cukic, B. (2010).** Estimating and fusing quality factors for iris biometric images. *IEEE Transactions on Systems, Man, and Cybernetics Part A: Systems and Humans*, 40(3), 509–524.
15. **Li, P., Liu, X., Xiao, L., & Song., Q. (2010).** Robust and accurate iris segmentation in very noisy iris images. *Image and Vision Computing*, 28(2), 246–253.
16. **Masek, L. (2003).** *Recognition of Human Iris Patterns for Biometric Identification*. Retrieved from www.csse.uwa.edu.au/~pk/studentprojects/libor/LiborMasekThesis.pdf
17. **Liu, X.M., Bowyer, K.W., & Flynn, P.J. (2005).** Experiments with an improved iris segmentation algorithm. *Fourth IEEE Workshop on Automatic Identification, Advanced Technologies*, Buffalo, NY, USA, 118–123.
18. **Deb, K. (2005).** Multi-Objective Optimization. In E. K. Burke & G. Kendall (Eds*.), Search Methodologies: introductory tutorials in optimization and decision support techniques*, (273–316), New York: Springer.
19. CASIA-IrisV4 Image Database Center for Biometrics and Security Research. (2010). Retrieved from http://biometrics.idealtest.org.
20. **Struc, V. & Pavesic, N. (2010).** The Complete Gabor-Fisher Classifier for Robust Face Recognition*. EURASIP Journal on Advances in Signal Processing*, 2010, Article No. 31.
21. **Sun, Z. & Tan, T. (2009).** Ordinal measures for iris recognition. *IEEE Transactions Pattern Analysis and Machine Intelligence*, 31(12), 2211–2226.

Yuniol Alvarez Betancourt graduated from the University of Cienfuegos in 2007 with a degree in Informatics Engineering. He received his M.Sc. degree in Computer Sciences from the University of Cienfuegos in 2010. The same year he received his Certificate of Advanced Studies from the University of Granada. He is currently a Ph.D. candidate at the University of Granada and Lecturer at the Computer Science Department of the University of Cienfuegos. His research interests include the fields of iris recognition, computer vision, pattern recognition and soft computing.

Miguel Garcia Silvente obtained a Ph.D. in Computer Science in 1996 and has been Lecturer at the Department of Computer Sciences and Artificial Intelligence of the University of Granada since 2000. He has more than 20 publications in international journals with impact factor in the field of computer vision. He works in human-robot interaction, active vision, fuzzy computer vision, biometrics, biomedical images, and robotics.

Article received on 30/04/2013, accepted on 14/07/2013..